THE JOURNAL OF BIOLOGICAL CHEMISTRY VOL. 290, NO. 11, pp. 6777–6788, March 13, 2015

Regulation of the Sarcoplasmic Reticulum Calcium Pump by Divergent Phospholamban Isoforms in Zebrafish*

Received for publication, May 29, 2014, and in revised form, January 13, 2015 Published, JBC Papers in Press, January 15, 2015, DOI 10.1074/jbc.M114.585604

Przemek A. Gorski[‡1], **Catharine A. Trieber**[‡§], **Ghazaleh Ashrafi**[‡2], **and Howard S. Young**[‡§3]

From the [‡]*Department of Biochemistry and* [§]*National Institute for Nanotechnology, University of Alberta, Edmonton, Alberta T6G 2H7, Canada*

Background: Zebrafish possess multiple phospholamban isoforms, one of which has a unique luminal domain.
Results: Zebrafish and human PLN have comparable effects on SERCA activity, and both can be reversed by phosphorylation.
Conclusion: Despite similar function, the zebrafish sequence variations are context-dependent and not synonymous with human phospholamban.
Significance: The different forms of phospholamban in zebrafish may provide a novel SERCA regulatory mechanism.

The sarcoplasmic reticulum calcium pump (SERCA) is regulated by the small integral membrane proteins phospholamban (PLN) and sarcolipin (SLN). These regulators have homologous transmembrane regions, yet they differ in their cytoplasmic and luminal domains. Although the sequences of PLN and SLN are practically invariant among mammals, they vary in fish. Zebrafish (zf) appear to harbor multiple PLN isoforms, one of which contains 18 sequence variations and a unique luminal extension. Characterization of this isoform (zfPLN) revealed that SERCA inhibition and reversal by phosphorylation were comparable with human PLN. To understand the sequence variations in zfPLN, chimeras were created by transferring the N terminus, linker, and C terminus of zfPLN onto human PLN. A chimera containing the N-terminal domain resulted in a mild loss of function, whereas a chimera containing the linker domain resulted in a gain of function. This latter effect was due to changes in basic residues in the linker region of PLN. Removing the unique luminal domain of zfPLN (^{53}SFHGM) resulted in loss of function, whereas adding this domain to human PLN had a minimal effect on SERCA inhibition. We conclude that the luminal extension contributes to SERCA inhibition but only in the context of zfPLN. Although this domain is distinct from the SLN luminal tail, zfPLN appears to use a hybrid PLN-SLN inhibitory mechanism. Importantly, the different zebrafish PLN isoforms raise the interesting possibility that sarcoplasmic reticulum calcium handling and cardiac contractility may be regulated by the differential expression of PLN functional variants.

The regulation of calcium transport across the sarcoplasmic reticulum (SR)[4] membrane plays a central role in the muscle contraction-relaxation cycle. Following the release of calcium from the SR during muscle contraction, the reuptake of calcium into the SR lumen determines the rate of relaxation as well as the amount of calcium available for subsequent contractions. Reuptake involves the active transport of calcium into the SR, which is accomplished by an ATP-dependent calcium pump (SERCA). In cardiac and smooth muscle, SERCA is regulated by phospholamban (PLN), a 52-amino acid integral membrane protein (1, 2). The interaction between SERCA and PLN is controlled by the β-adrenergic pathway, where the phosphorylation of PLN by cAMP-dependent protein kinase (PKA) reverses SERCA inhibition and modulates the overall SR calcium load (3). In fast-twitch skeletal muscle and the atria of the heart, SERCA is regulated by sarcolipin (SLN), a 31-amino acid homolog of PLN (4, 5). There is a high degree of sequence homology in the transmembrane regions of PLN and SLN, suggesting a similar mode of interaction with SERCA (6, 7). Although studies have demonstrated that PLN and SLN use distinct structural elements and mechanisms to regulate SERCA (8, 9), crystal structures of the SERCA-SLN (10, 11) and SERCA-PLN (12) complexes are remarkably similar to one another.

The topology of PLN is organized into three domains as follows: an α-helical cytoplasmic domain (residues 1–20), a linker domain (residues 21–30), and an α-helical transmembrane domain (residues 31–52) (13–16). The cytoplasmic domain makes a small contribution to SERCA inhibition, yet it has two phosphorylation sites (Ser^{16} and Thr^{17}) that play a critical role in the regulation of PLN inhibitory function. Indeed, several hereditary mutations in this domain are associated with early-onset, lethal heart failure in humans (17–19). The linker domain of PLN can also interact with SERCA, although residues such as Lys^{27}, Gln^{29}, and Asn^{30} appear to modulate the physical interaction with SERCA rather than making a direct contribution to inhibition (20). Finally, the transmembrane domain of PLN encodes most of its inhibitory properties, which

* This work was supported in part by a grant from Heart and Stroke Foundation of Canada.
[1] Supported by Canada Graduate Scholarships from Canadian Institutes of Health Research and Alberta Innovates-Technology Futures. Present address: Cardiovascular Research Center, Icahn School of Medicine, Mount Sinai Hospital, New York, NY 10029.
[2] Present address: Dept. of Biochemistry, Weill Cornell Medical College, New York, NY 10065.
[3] To whom correspondence should be addressed: Medical Sciences Building, Rm. 327, University of Alberta, Edmonton, Alberta T6G 2H7, Canada. Tel.: 780-492-3931; Fax: 780-492-0886; E-mail: hyoung@ualberta.ca.

[4] The abbreviations used are: SR, sarcoplasmic reticulum; SERCA, sarcoplasmic reticulum calcium ATPase; PLN, phospholamban; SLN, sarcolipin; zfPLN, zebrafish PLN; PKA, protein kinase A.

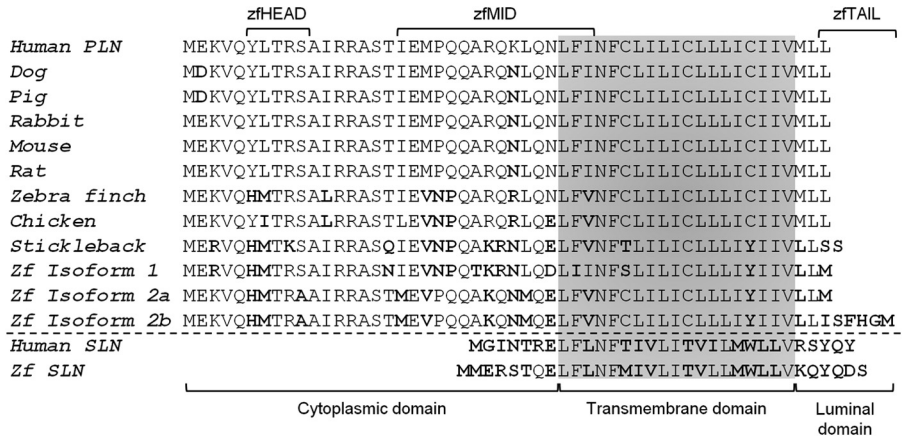

FIGURE 1. **Sequence alignments for primary structures of PLN and SLN from representative species.** There are three zebrafish PLN isoforms (isoform 1, UniProt X1WCE4; isoform 2a, UniProt E7F215; and isoform 2b, NCBI NM_001201561). Herein, zebrafish PLN isoform 2b is referred to as zfPLN. The cytoplasmic, transmembrane, and luminal domains are indicated. Sequence variations, as compared with human PLN, are indicated in *boldface*. The three clusters of sequence variation (zfHEAD, zfMID, and zfTAIL) are indicated.

manifest as a decrease in the apparent calcium affinity of SERCA (21, 22). The PLN transmembrane domain is highly hydrophobic and contains residues that are either critical for inhibitory function (*e.g.* Leu^{31} and Asn^{34}) or involved in self-association to form a pentamer (leucine-isoleucine zipper) (23, 24). Comparatively, SLN has a short cytoplasmic domain (residues 1–7), a transmembrane domain homologous to that of PLN (residues 8–26), and a short, unique luminal domain (residues 27–31). Like PLN, the cytoplasmic domain of SLN is involved in regulating the interaction with SERCA (25, 26). However, unlike PLN, much of the inhibitory activity of SLN relies on its unique luminal domain rather than its transmembrane domain alone (8).

Because of its role in the heart, most structural and functional studies of PLN have concentrated on its mammalian forms. Nevertheless, PLN is found in many nonmammalian vertebrates, including birds, amphibians, and fish (27, 28). This ubiquitous expression emphasizes the importance of PLN as a regulator of calcium transport in cardiac muscle of many organisms. There is a remarkable degree of sequence homology between the mammalian forms of PLN with mainly as few as one or two amino acid substitutions between them all. In birds and fish, however, PLN shows much greater divergence. For example, chicken and zebrafish PLN are 83 and 68% identical to human PLN, respectively. Indeed, sequences have been reported for three zebrafish PLN isoforms (Fig. 1), and compared with human PLN, isoform 2b (referred to as zfPLN herein) contains 13 sequence variations and five additional residues at the C terminus. Most of the residue differences between human and zfPLN cluster in three distinct regions, suggesting that these more complex sequence changes could alter PLN function. The most intriguing variation in zfPLN is the addition of a C-terminal tail (residues 53–57). Unlike other PLN proteins, zfPLN has an additional five amino acids that extend into the SR lumen (Fig. 1). It is important to note that the C-terminal sequence of PLN in all mammals and birds is perfectly conserved (Met^{50}-Leu-Leu^{52}). In zfPLN, this sequence is modified to the longer and more polar Leu^{50}-Leu-Ile-Ser-Phe-His-Gly-Met^{57}, with the last five residues being reminiscent of the luminal Arg^{27}-Ser-Tyr-Gln-Tyr^{31} sequence of SLN. So far, it is not known whether zfPLN can regulate SERCA and whether this regulation resembles that of human PLN or SLN.

Given the high sequence diversity between zebrafish and human PLN, as well as the presence of a unique zfPLN luminal extension, we characterized the ability of zfPLN to regulate SERCA. We found that zebrafish and human PLN have comparable effects on SERCA activity and that both can be reversed by PKA-mediated phosphorylation of PLN. Human PLN chimeras containing regions of the zfPLN sequence resulted in altered SERCA inhibition. Thus, despite similar function, the zebrafish sequence variations are context-dependent and not synonymous with human PLN. Further study of the unique luminal domain of zfPLN indicated that it contributes to SERCA inhibition; however, this domain is not functional when transferred to human PLN, and it cannot be replaced with the SLN luminal tail. We conclude that the luminal extension of zfPLN is a distinct structural element and that zfPLN has characteristics reminiscent of both PLN and SLN.

EXPERIMENTAL PROCEDURES

Expression and Purification of PLN—Human and zebrafish (*Danio rerio*; isoforms 2b) PLN variants were expressed and purified as described previously (29). Mutants were confirmed by DNA sequencing (TAGC Sequencing, University of Alberta) and by MALDI-TOF mass spectrometry (Institute for Biomolecular Design, University of Alberta). To phosphorylate PLN, detergent-solubilized PLN was treated with the catalytic subunit of PKA (Sigma) (30).

Co-reconstitution of SERCA and PLN—Established procedures were used to purify SERCA1a from rabbit skeletal muscle (31, 32) and SERCA2a from porcine cardiac muscle (33). SERCA1a (30) and SERCA2a (33) were then reconstituted into proteoliposomes with PLN. The co-reconstituted proteoliposomes typically yielded final molar stoichiometries of 1 SERCA to 4.5 PLN. The SERCA and PLN concentrations were determined by BCA assay and quantitative SDS-PAGE (34).

Activity Assays—Calcium-dependent ATPase activities of the co-reconstituted proteoliposomes were measured by a coupled enzyme assay (35). The coupled enzyme assay reagents were of the highest purity available (Sigma). All co-reconsti-

tuted peptide constructs were compared with a negative control (SERCA reconstituted in the absence of PLN) and a matched positive control (SERCA co-reconstituted in the presence of either wild-type human PLN or zebrafish PLN isoform 2b). A minimum of three independent reconstitutions and activity assays were performed for each peptide, and the calcium-dependent ATPase activity was measured over a range of calcium concentrations (0.1 to 10 μM) for each assay. This method has been described in detail (30). The K_{Ca} (calcium concentration at half-maximal activity), the V_{max} (maximal activity), and the n_H (Hill coefficient) values were calculated based on nonlinear least squares fitting of the activity data to the Hill equation using SigmaPlot software (SPSS Inc., Chicago). Errors were calculated as the standard error of the mean for a minimum of three independent measurements. Comparison of K_{Ca}, V_{max}, and n_H parameters was carried out using analysis of variance (between subjects, one-way analysis of variance) followed by the Holm-Sidak test for pairwise comparisons (SigmaPlot).

Kinetic Simulations—Reaction rate simulations have been used to describe the transport cycle of SERCA in the absence and presence of PLN (36, 37) and SLN (8), and we have adopted this approach to understand SERCA inhibition by zfPLN. Based on reaction rate constants determined for the transport cycle of SERCA (21, 38), we performed a global nonlinear regression fit of the model to each plot of SERCA ATPase activity *versus* calcium concentration using Dynafit (BioKin Ltd., Watertown, MA). An underlying assumption is that the rate constants (21, 38) are a valid starting model for the kinetic simulations and that these values are close to the correct solution for SERCA in the presence of regulatory peptides. In optimizing the fit for SERCA in the presence of regulatory peptides, all reaction steps were initially allowed to vary. In this initial fit, rate constants that did not change more than the average error (in the kinetic simulations) were held at the starting model value. Each of the remaining rate constants were systematically varied to test whether they improved the fit to the experimental data (based on the sum of squared residuals). Rate constants that did not improve the fit to the experimental data were held at the starting model value. For the final fit, the remaining rate constants (typically 2–4 rate constants) were allowed to vary to minimize the discrepancy between the experimental data and the kinetic model. The starting points for the kinetic simulations included global fits previously reported for the following: (i) SERCA alone (38), (ii) SERCA in the presence of wild-type PLN (21, 36), and (iii) SERCA in the presence of wild-type SLN (8). Errors were calculated as the standard error of the mean based on standard deviations calculated by Dynafit. A one-sample *t* test was used to evaluate the statistical significance of individual rate constants *versus* previously determined values (8, 21, 36, 38).

RESULTS

Human Versus Zebrafish PLN—Herein we focused primarily on SERCA1a in the presence of human and zebrafish PLN; however, we also tested zfPLN in the presence of the cardiac SERCA2a isoform. Unless explicitly stated, we use the terms "SERCA" to designate the SERCA1a isoform and "zfPLN" to designate zebrafish PLN isoform 2b.

SERCA was co-reconstituted into proteoliposomes in the absence and presence of zfPLN. The co-reconstitution procedure has been described in detail (29, 30, 36, 37, 39–41). The final molar ratio in the proteoliposomes was 1 SERCA to 4.5 zfPLN to 120 lipids, and there was no observable difference in the reconstitution efficiency of human *versus* zebrafish PLN. PLN is known to form pentamers observable by SDS-PAGE (2), and similar behavior was observed for zfPLN (Fig. 2). With these proteoliposomes, the calcium-dependent ATPase activity of SERCA was measured, where SERCA reconstituted in the presence of human PLN served as a positive control. Under these conditions, proteoliposomes containing SERCA alone yielded an apparent calcium affinity (K_{Ca}) of 0.46 μM and a maximal activity (V_{max}) of 4.1 μmol mg^{-1} min^{-1} (Table 1). Inclusion of human PLN in proteoliposomes decreased the apparent calcium affinity (0.88 μM calcium; ΔK_{Ca} of 0.42) and increased the maximal activity (6.1 μmol mg^{-1} min^{-1}; ΔV_{max} of 2.2) of SERCA. Incorporation of zfPLN into proteoliposomes with SERCA resulted in a K_{Ca} value similar to that for human PLN (0.85 μM calcium; ΔK_{Ca} of 0.39) and a slightly higher V_{max} value (6.9 μmol mg^{-1} min^{-1}; ΔV_{max} of 2.8). Thus, despite the sequence variation in zfPLN, it had regulatory properties similar to human PLN. A similar approach was used to study the effects of human and zebrafish PLN on SERCA2a, and there was no discernible difference in their regulatory properties (Fig. 3).

A hallmark of mammalian PLNs is the ability to reverse SERCA inhibition by PKA-mediated phosphorylation at Ser^{16} (2, 42). To test this, we phosphorylated zfPLN with PKA followed by co-reconstitution into proteoliposomes with SERCA (43). As expected, phosphorylation of zfPLN reduced the apparent calcium affinity of SERCA to near control levels (Table 1; K_{Ca} values of 0.55 and 0.46 μM calcium, respectively). This compared well with findings for human PLN, where phosphorylation resulted in complete reversal of SERCA inhibition (K_{Ca} of 0.45 μM) (30, 41).

Functional Contributions of Zebrafish PLN Sequence Variation—The primary structural variations in zfPLN can be grouped into three distinct regions (designated zfHEAD, zfMID, and zfTAIL), as well as three transmembrane residue changes at Tyr^{46}, Leu^{50}, and Ile^{52} (Fig. 2). Each of the three regions contains a cluster of residues that differ from the human PLN sequence. There are three residue changes in the N-terminal helix (Tyr^6 to His, Leu^7 to Met, and Ser^{10} to Ala), seven residue changes in the linker region (Ile^{18} to Met, Met^{20} to Val, Arg^{25} to Lys, Lys^{27} to Asn, Leu^{28} to Met, Asn^{30} to Glu, and Ile^{33} to Val), and five residues added to the C terminus (Ser^{53}-Phe-His-Gly-Met^{57}). Although many of the residue changes are conservative, they represent more global sequence variations compared with the traditional alanine-scanning mutagenesis that has been used to study PLN function (20, 24, 36, 37). To investigate the functional consequences of these sequence variations, we created chimeric peptides that consisted of human PLN containing each of the zebrafish regions.

We first focused on the cytoplasmic domain chimeras (zfHEAD and zfMID) and a single residue change in the trans-

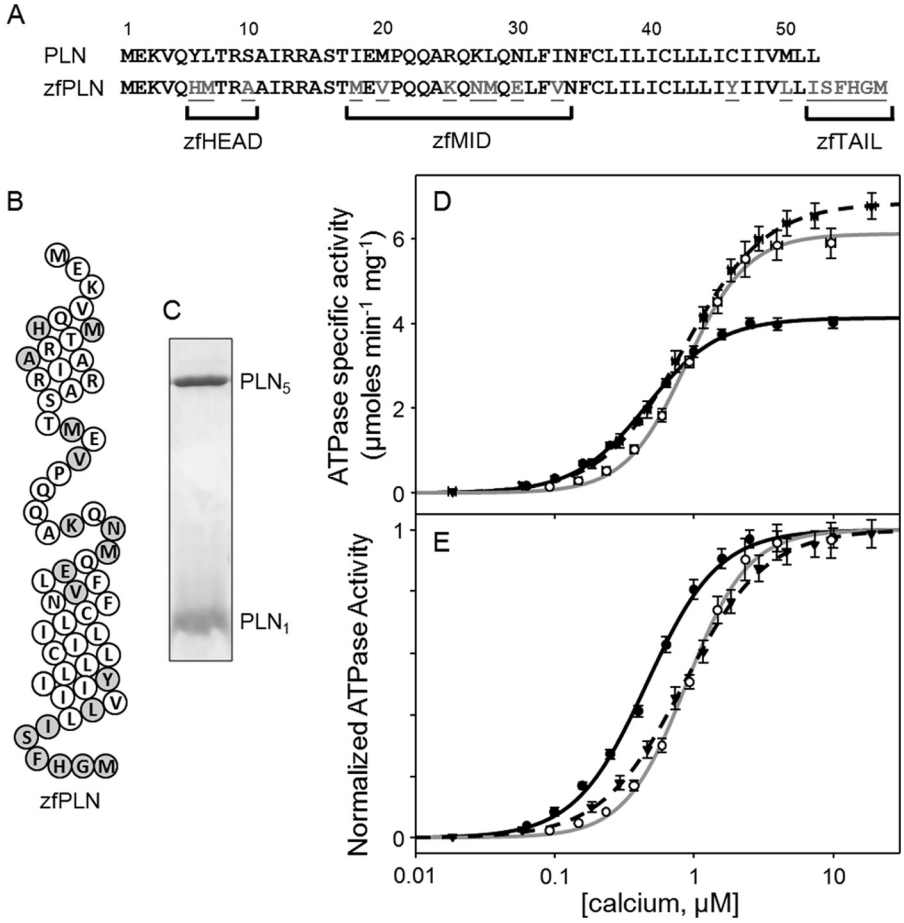

FIGURE 2. **Functional data for wild-type human and zebrafish PLN co-reconstituted into proteoliposomes with SERCA1a.** *A,* sequence alignment for human and zebrafish PLN. The differences in sequence composition are *underlined*, and the three clusters of sequence variation (zfHEAD, zfMID, and zfTAIL) are indicated with *brackets*. *B,* topology model for zfPLN. *C,* SDS-PAGE of zfPLN (5 μg of protein; 16% gel). Pentameric and monomeric zfPLN are indicated. Shown are ATPase activity (*D*) and normalized ATPase activity (*E*) as a function of calcium concentration for SERCA alone (*solid black line*), SERCA in the presence of wild-type human PLN (*solid gray line*), and SERCA in the presence of zfPLN (*dashed line*). The V_{max}, K_{Ca}, and n_H values are given in Table 1. Each data point is the mean ± S.E. (*error bars*) ($n \geq 3$).

membrane domain (Cys[46] to Tyr; Fig. 4 and Table 1). The calcium-dependent ATPase activity was measured for SERCA in the presence of each peptide. Inclusion of the zfHEAD chimera in proteoliposomes with SERCA resulted in a similar increase in K_{Ca} as seen for human PLN (K_{Ca} values of 0.94 and 0.88 μM, respectively). Surprisingly, the zfHEAD chimera did not increase the maximal activity of SERCA. Compare V_{max} values for SERCA alone (4.1 μmol mg^{-1} min^{-1}), SERCA in the presence of zfHEAD (4.3 μmol mg^{-1} min^{-1}), SERCA in the presence of human PLN (6.1 μmol mg^{-1} min^{-1}), and SERCA in the presence of zfPLN (6.9 μmol mg^{-1} min^{-1}). Next, we tested the zfMID chimera in proteoliposomes with SERCA. Compared with human PLN, the zfMID chimera was a super-inhibitor of SERCA (K_{Ca} values of 0.88 and 1.1 μM calcium, respectively), while maintaining the characteristic increase in maximal activity (Table 1). Finally, the Cys[46] to Tyr mutation had a small effect on the ability of human PLN to alter the apparent calcium affinity (K_{Ca} values of 0.89 and 0.88 μM, respectively) and maximal activity of SERCA (V_{max} values of 6.6 and 6.1 μmol mg^{-1} min^{-1}, respectively). However, the Cys[46] to Tyr substitution resulted in a monomeric variant of human PLN by SDS-PAGE (data not shown), despite the fact that both human and zebrafish PLN can form pentamers.

Functional Contributions of the Zebrafish Tail—A distinctive feature of zfPLN is the C-terminal luminal domain (Ser[53]-Phe-His-Gly-Met[57]), which is lacking in all other known PLN sequences. Although SLN contains a luminal domain that contributes to SERCA inhibition (4, 8, 44), the key question was whether or not the luminal extension of zfPLN contributes to its inhibitory properties. We created two truncation variants of zfPLN, one with the last five C-terminal residues removed and another with the last six residues removed (designated zfPLN(−5) and zfPLN(−6), respectively; Fig. 5). It should be mentioned that removal of the luminal tail did not affect the ability of either of the truncated peptides to form pentamers by SDS-PAGE (data not shown). Inclusion of zfPLN(−5) in proteoliposomes resulted in a moderate loss of SERCA inhibition (K_{Ca} of 0.70 μM calcium; 62% of zfPLN inhibitory capacity), and its effect on V_{max} did not significantly differ from that of zfPLN (Table 1). The zfPLN(−6) truncation behaved in a similar manner, with a K_{Ca} of 0.67 μM calcium (54% of zfPLN inhibitory capacity). Thus, the luminal extension of zfPLN appeared to encode ~40% of its inhibitory activity. This contrasts with what is known for PLN and SLN, where the inhibitory activity of PLN is encoded by its transmembrane domain (~80% (37)), and the inhibitory activity of SLN depends on its luminal tail (~75%

TABLE 1

Kinetic parameters for SERCA in the absence and presence of phospholamban variants

The following abbreviations are used: hPLN, human phospholamban; hSLN, human sarcolipin; ph-hPLN, phosphorylated hPLN; zfPLN, zebrafish PLN isoform 2b; ph-zfPLN, phosphorylated zfPLN; zfHEAD, hPLN chimera containing the three-residue changes in the N-terminal helix of zfPLN (Tyr^{6} to His, Leu^{7} to Met, and Ser^{10} to Ala); zfMID, hPLN chimera containing the 7-residue changes in the linker region of zfPLN (Ile^{18} to Met, Met^{20} to Val, Arg^{25} to Lys, Lys^{27} to Asn, Leu^{28} to Met, Asn^{30} to Glu, and Ile^{33} to Val); C46Y, hPLN containing a Cys^{46} to Tyr substitution; zfPLN(−5), zfPLN lacking last five residues; zfPLN(−6), zfPLN lacking last six residues; hPLN(+5), hPLN chimera containing the last five residues of zfPLN; hPLN(+6), hPLN chimera containing the last six residues of zfPLN; zfPLN-SLN$_{tail}$, zfPLN chimera containing the last five residues of SLN; F54A, Phe^{54} to Ala mutant of zfPLN; H55A, His^{55} to Ala mutant of zfPLN; F54A,H55A, double mutant. For statistical analysis, between subjects one-way analysis of variance followed by the Holm-Sidak test was used for pairwise comparisons against SERCA in the absence and presence of wild-type human PLN.

	V_{max}	K_{Ca}	n_H	n
	$\mu mol\ mg^{-1}\ min^{-1}$	μM		
SERCA	4.1 ± 0.1	0.46 ± 0.02	1.7 ± 0.1	32
hSLN	2.9 ± 0.1[a,b]	0.80 ± 0.02[a,b]	1.4 ± 0.1	10
hPLN	6.1 ± 0.1[a]	0.88 ± 0.03[a]	2.0 ± 0.1	9
ph-hPLN	6.3 ± 0.1[a]	0.45 ± 0.02[b]	1.7 ± 0.1	4
zfPLN	6.9 ± 0.1[a,b]	0.85 ± 0.01[a]	1.5 ± 0.1	12
ph-zfPLN	5.6 ± 0.1[a]	0.55 ± 0.01[b]	1.7 ± 0.1	3
zfHEAD	4.3 ± 0.1[b]	0.94 ± 0.04[a]	1.6 ± 0.1	7
zfMID	5.9 ± 0.1[a,b]	1.1 ± 0.05[a,b]	1.4 ± 0.1	8
C46Y	6.6 ± 0.1[a,b]	0.89 ± 0.03[a]	1.6 ± 0.1	4
zfPLN (−5)	7.2 ± 0.1[a,b]	0.70 ± 0.03[a,b]	1.6 ± 0.1	8
zfPLN (−6)	6.4 ± 0.1[a]	0.67 ± 0.03[a,b]	1.6 ± 0.1	6
hPLN (+5)	5.7 ± 0.1[a,b]	0.94 ± 0.02[a,b]	1.6 ± 0.1	8
hPLN (+6)	6.8 ± 0.1[a,b]	0.76 ± 0.02[a,b]	1.6 ± 0.1	6
zfPLN-SLN$_{tail}$	4.7 ± 0.1[a,b]	1.5 ± 0.06[a,b]	2.0 ± 0.1	5
F54A	6.1 ± 0.1[a]	1.10 ± 0.02[a,b]	1.7 ± 0.1	3
H55A	7.0 ± 0.1[a]	1.02 ± 0.02[a,b]	1.4 ± 0.1	3
F54A,H55A	5.8 ± 0.1[a]	1.58 ± 0.02[a,b]	1.8 ± 0.1	2

[a] $p < 0.05$ compared with SERCA in the absence of wild-type human or zebrafish PLN.

[b] $p < 0.05$ compared with SERCA in the presence of wild-type human PLN.

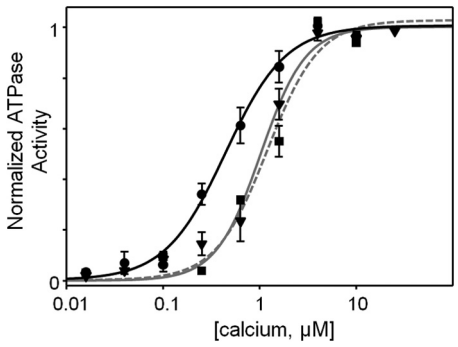

FIGURE 3. **Functional data for wild-type human and zebrafish PLN co-reconstituted into proteoliposomes with SERCA2a.** Shown are normalized ATPase activities as a function of calcium concentration for SERCA2a alone (*solid black line*), SERCA in the presence of human PLN (*inverted triangles*, *solid gray line*), and SERCA in the presence of zfPLN (*squares*, *dashed gray line*). The K_{Ca} values for human and zebrafish PLN were indistinguishable from one another (1.2 ± 0.1 μM calcium; $n = 3$).

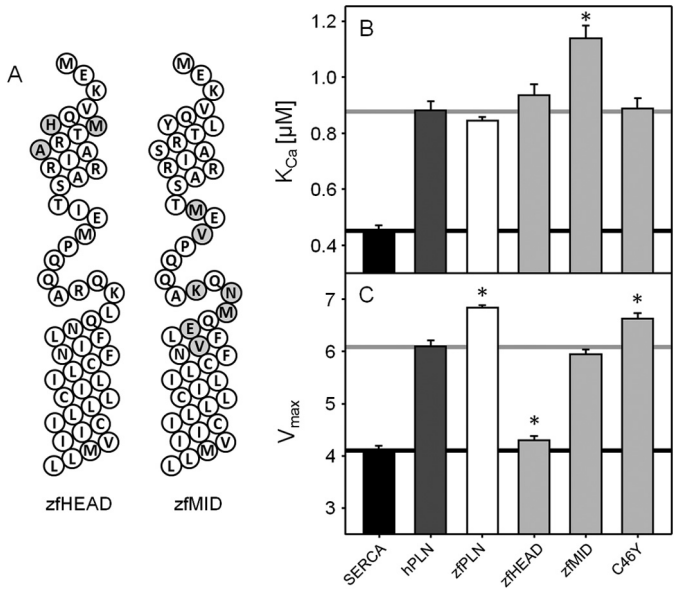

FIGURE 4. **Cytoplasmic and transmembrane human-zebrafish PLN chimeras.** *A*, topology model for zfHEAD and zfMID chimeras (*white*, conserved residues; *gray*, variant zebrafish PLN residues). K_{Ca} (*B*) and V_{max} (*C*) values were determined from ATPase activity measurements for SERCA in the absence and presence of zfHEAD, zfMID, and C46Y chimeras. Each data point is the mean ± S.E. (*error bars*) ($n \geq 4$). The V_{max}, K_{Ca}, and n_H are given in Table 1. *Asterisks* indicate comparisons against SERCA in the presence of wild-type human PLN ($p \geq 0.05$).

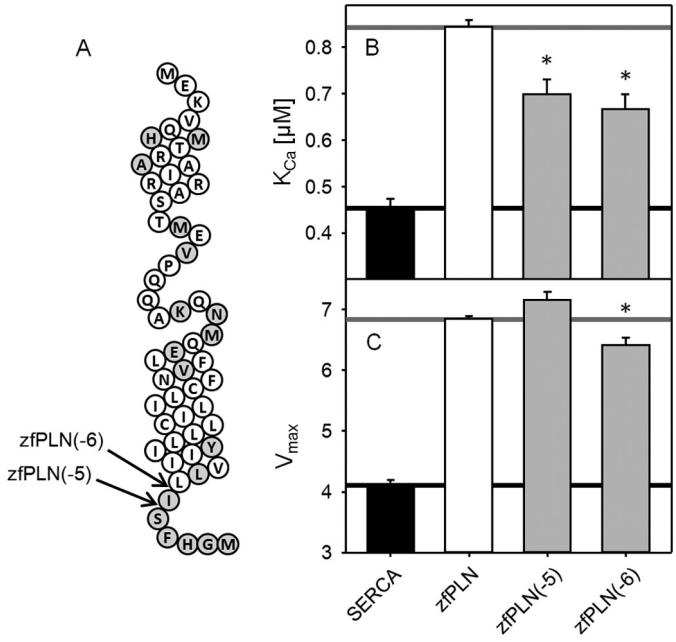

FIGURE 5. **Removal of the zfPLN luminal tail.** *A*, topology model for zfPLN with the truncation sites for zfPLN (−5) and zfPLN (−6) indicated with *arrows* (*white*, conserved residues; *gray*, variant zfPLN residues). K_{Ca} (*B*) and V_{max} (*C*) values were determined from ATPase activity measurements for SERCA in the absence and presence of zfPLN (−5) and zfPLN (−6) truncation variants. Each data point is the mean ± S.E. (*error bars*) ($n \geq 4$). The V_{max}, K_{Ca}, and n_H values are given in Table 1. *Asterisks* indicate comparisons against SERCA in the presence of zfPLN ($p \geq 0.05$).

(8)). Nonetheless, there is an interesting parallel between the luminal extensions of zfPLN and SLN in that they both contribute to SERCA inhibition, albeit with different magnitudes of SERCA inhibition (~40% *versus* ~75%, respectively).

A characteristic of the SLN luminal tail is that it is a distinct and transferable SERCA regulatory domain (8). When transferred to human PLN, a chimera containing the SLN luminal tail resulted in super-inhibition of SERCA. To characterize this behavior for the zfPLN tail, we generated three chimeric constructs. The first chimera contained the last five residues of zfPLN added to the C terminus of human PLN and the second chimera contained the last six residues (designated hPLN(+5) and hPLN(+6), respectively; Fig. 6). In co-reconstituted proteoliposomes with SERCA, these two chimeras resulted in only minor changes in the apparent calcium affinity and maximal

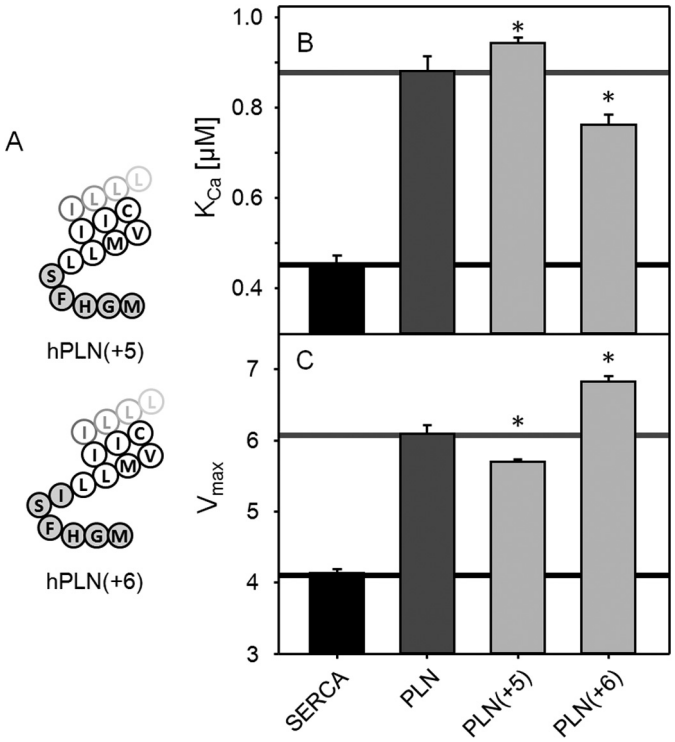

FIGURE 6. **Transferring the luminal tail of zfPLN to human PLN.** *A,* topology models of hPLN (+5) and hPLN (+6) chimeras (*white*, human PLN residues; *gray*, zebrafish PLN luminal residues). K_{Ca} (*B*) and V_{max} (*C*) values were determined from ATPase activity measurements for SERCA in the absence and presence of hPLN (+5) and hPLN (+6) variants. Each data point is the mean ± S.E. (*error bars*) ($n \geq 4$). The V_{max}, K_{Ca}, and n_H are given in Table 1. *Asterisks* indicate comparisons against SERCA in the presence of wild-type human PLN ($p \geq 0.05$).

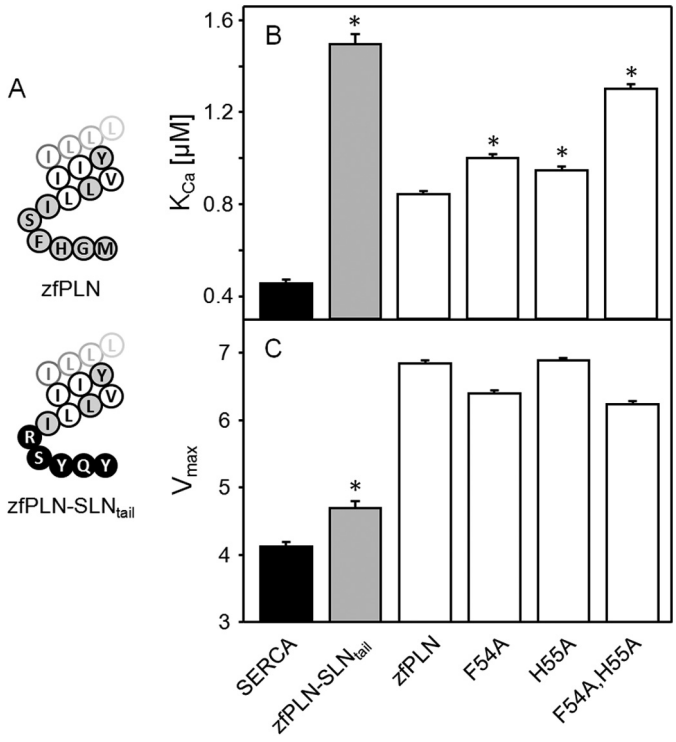

FIGURE 7. **Replacing the luminal tail of zfPLN with the luminal tail of human SLN, and mutagenesis of the luminal tail of zfPLN.** *A,* topology model for wild-type zfPLN and zfPLN-hSLN$_{tail}$ (*white*, conserved PLN residues; *gray*, variant zebrafish PLN residues; *black*, human SLN luminal domain). K_{Ca} (*B*) and V_{max} (*C*) values were determined from ATPase activity measurements for SERCA in the absence and presence of zfPLN-hSLN$_{tail}$ chimera and zfPLN alanine mutants (F54A, Phe^{54} to Ala; H55A, His^{55} to Ala; and the double mutant F54A,H55A). Each data point is the mean ± S.E. (*error bars*) ($n \geq 4$). The V_{max}, K_{Ca}, and n_H are given in Table 1. *Asterisks* indicate comparisons against SERCA in the presence of wild-type zebrafish PLN ($p \geq 0.05$).

activity of SERCA as compared with human PLN (Table 1). Thus, unlike SLN, the luminal domain of zfPLN did not retain inhibitory function when transferred to human PLN. In the third chimera we tested, the luminal domain of zfPLN was substituted with that from SLN (^{27}RSYQY added after Ile^{52} of zfPLN; designated zfPLN-SLN$_{tail}$; Fig. 7). If a functional parallel exists between these two luminal domains, we might expect this chimera to have normal zfPLN function. However, if these domains are distinct, we would expect to observe the super-inhibition of SERCA reported previously for a human PLN-SLN chimera (8). Including zfPLN-SLN$_{tail}$ in the proteoliposomes resulted in potent super-inhibition of SERCA (K_{Ca} of 1.5 μM) and only a small increase in the maximal activity of SERCA (V_{max} value of 4.7 μmol mg^{-1} min^{-1}). Because these are SLN-like qualities, it led us to conclude that the luminal domain of zfPLN has a distinct regulatory function that cannot be replaced by the luminal domain of human SLN.

Mutagenesis of the Zebrafish Luminal Domain—Aromatic residues play a key role in regulating SERCA from the luminal side of the SR membrane, as observed for the luminal domain of SLN (4, 8, 44) and the C-terminal tail of the ubiquitous SERCA2b splice variant (45, 46). For this reason, we focused on the role of Phe^{54} and His^{55} in the luminal tail of zfPLN. We substituted alanine residues at these positions in the wild-type zfPLN sequence (Phe^{54} to Ala, His^{55} to Ala, and the double mutant) and co-reconstituted the mutant peptides into proteoliposomes with SERCA. Calcium-dependent ATPase activity measurements revealed that mutation of one or both residues resulted in super-inhibition of SERCA (the K_{Ca} values were 1.10, 1.02, and 1.58 μM, respectively; Table 1 and Fig. 7). At first glance, the observed super-inhibition may seem counterintuitive. Tyr^{31} of SLN and Phe^{54} of zfPLN are at homologous positions (Fig. 1), yet the alanine substitutions have opposite effects (Table 1) (8). However, the sequence of zfPLN's luminal extension extends further into the SR lumen, and it forms a distinct structural element compared with the SLN tail. Importantly, zfPLN's luminal extension must enable a precise level of SERCA inhibition over the calcium concentrations required for normal cardiovascular function. The potent inhibition observed for the alanine mutants (Phe^{54} to Ala, His^{55} to Ala, and the double mutant; Table 1) and the SLN tail chimera (zfPLN-SLN$_{tail}$; Fig. 7) suggests that the luminal extension of zfPLN has selectively evolved to avoid super-inhibition of SERCA.

Kinetic Simulations for Zebrafish PLN—From the above results, it is clear that the luminal domain of zfPLN contributes to its inhibitory function in a manner that is distinct from other vertebrate forms of PLN and SLN. To gain insight into this mechanistic difference, we used kinetic reaction rate simulations to describe calcium transport by SERCA in the absence and presence of zfPLN. In the simulated reaction scheme, calcium binding to SERCA occurs as two steps linked by a conformational change that establishes cooperativity (Fig. 8; E +

$$E + Ca \underset{A_{rev}}{\overset{A_{for}}{\rightleftharpoons}} ECa \underset{B_{rev}}{\overset{B_{for}}{\rightleftharpoons}} E'Ca + Ca \underset{C_{rev}}{\overset{C_{for}}{\rightleftharpoons}} E'CaCa$$

FIGURE 8. **Partial reaction scheme for calcium transport by SERCA.** Calcium binding involves three distinct steps (21, 38) as follows: binding of the first calcium ion (A_{for} and A_{rev}), a conformational change that establishes cooperativity (B_{for} and B_{rev}), and binding of the second calcium ion (C_{for} and C_{rev}).

$Ca \leftrightarrow ECa \leftrightarrow E'Ca + Ca \leftrightarrow E'2Ca$) (21, 36). Kinetic simulations for human PLN revealed that it primarily affects the SERCA conformational change ($ECa \leftrightarrow E'Ca$; rate constants B_{for} and B_{rev}). This manifests as a decrease in the apparent calcium affinity of SERCA and an increase in cooperativity for binding of the second calcium ion. Kinetic simulations for human SLN revealed that it uses a different mechanism (8). Although SLN also targets the SERCA conformational transition ($ECa \leftrightarrow E'Ca$; B_{for} and B_{rev}), the primary effect is on binding of the first calcium ion ($E + Ca \leftrightarrow ECa$; A_{for} and A_{rev}).

What is the mechanism used by zfPLN? Despite having a primary structure that is largely homologous to human PLN, performing the kinetic simulations for zfPLN (Table 2) revealed that its mechanism of regulating SERCA more closely resembles that used by SLN. Effects were observed on both binding of the first calcium ion to SERCA ($E + Ca \leftrightarrow ECa$; increase in A_{rev}), as well as the SERCA conformational change ($ECa \leftrightarrow E'Ca$; increase in B_{rev}). However, there was one major difference between zfPLN and SLN. Human PLN and zfPLN increase the maximal activity of SERCA, whereas SLN decreases the maximal activity (Table 1). These changes in maximal activity occur through a shift in the equilibrium for the SERCA conformational change ($ECa \rightarrow E'Ca$; increase or decrease in B_{for}, respectively). Although the SERCA conformational change is not the rate-limiting step in the reaction cycle, it is the slowest step in calcium binding (21). Nonetheless, the effect of zfPLN on binding of the first calcium ion to SERCA is a SLN-like trait attributable to its luminal domain. To test this notion, we performed the kinetic simulations on zfPLN lacking the five luminal residues (zfPLN(−5); Fig. 5 and Table 2). The expectation was that the SLN-like effect on binding of the first calcium ion to SERCA ($E + Ca \leftrightarrow ECa$; increase in A_{rev}) should be reversed by removal of this domain. Indeed, we found that A_{rev} was reduced, indicating that the luminal domain of zfPLN was responsible for this effect.

DISCUSSION

Of Humans, Rabbits and Zebrafish—The goal of this study was to examine functional differences between human and zebrafish PLN in reconstituted proteoliposomes with SERCA. We used an *in vitro* reconstitution system that is designed to mimic cardiac SR membranes while offering the opportunity for detailed mechanistic insights (30, 36, 37, 41). However, this system uses rabbit skeletal muscle SERCA1a as an effective substitute for the cardiac-specific isoform SERCA2a (33). Although we also examined human and zebrafish PLN in proteoliposomes with porcine cardiac muscle SERCA2a (Fig. 3), it is important to recognize that our primary focus was on human and zebrafish PLN and rabbit SERCA1a. Thus, the primary structure of zfPLN could simply reflect compensatory sequence changes in response to the primary structure of zebrafish SERCAs. In other words, sequence differences between rabbit SERCA1a and zebrafish SERCA2a might account for the functional differences observed with zfPLN. To consider this, we mapped sequence variations for human and zebrafish SERCA2a onto the structure of rabbit SERCA1a (Fig. 9). Rabbit SERCA1a, human SERCA2a, and zebrafish SERCA2a have ~85% identical amino acid sequences. The differences localize to the surface of the protein, and there are no sequence variations in the PLN binding groove on SERCA (M2, M6, and M9 (10)). This indicates that differences between human, rabbit, and zebrafish SERCA isoforms cannot account for our functional results.

Human Versus Zebrafish PLN—The primary structure of PLN is practically invariant in mammals, with typical sequence variations at one or two residue positions (*e.g.* Glu^2 to Asp and Lys^{27} to Asn). However, nonmammalian vertebrates have considerable sequence variation with as many as 18 residues differing from the human PLN sequence. Zebrafish contain two genes for PLN (Fig. 1), isoform 1 on chromosome 17 and isoform 2 on chromosome 20 (two variants of isoform 2 have been reported). The primary difference between the two isoforms is the C-terminal extension present in isoform 2b (designated zfPLN herein). Transcripts (cDNA) encoding these proteins have been found in a variety of zebrafish tissues, including the heart (UniGene Dr.76091). We decided to functionally characterize zfPLN because it has the highest sequence variation among the known PLN genes, and it has a unique luminal extension that could be involved in SERCA regulation. In addition, nonmammalian PLNs have not been studied, and many of them contain sequence variations in the same regions of the protein. Because this is the first detailed characterization of a nonmammalian form of PLN, we wanted to understand whether there are differences in how PLN from lower organisms regulates SERCA activity. Because PLN is a major determinant of cardiac contractility, we wished to identify structural elements that differentiate human PLN from a nonmammalian ortholog.

Incorporating zfPLN into proteoliposomes with SERCA, we found that it altered the apparent calcium affinity of SERCA to an equivalent degree as human PLN (Fig. 2 and Table 1). This inhibition was reversed by PKA-mediated phosphorylation, confirming that zfPLN can respond to β-adrenergic stimulation. This led us to conclude that despite the high sequence variations between zebrafish and human PLN, they have remarkably similar physical and functional characteristics.

Zebrafish HEAD—Considering the different regions of PLN as distinct structural elements, we first investigated three sequence variations in the N-terminal α-helix of zfPLN (Tyr^6 to His, Leu^7 to Met, and Ser^{10} to Ala; Fig. 4). The zfHEAD chimera retained the ability to inhibit SERCA (Table 1). Perhaps this is not surprising given the conservative nature of the amino acid changes. However, unlike human and zfPLN, the chimera was unable to stimulate the maximal activity of SERCA. In previous studies of human PLN, alanine substitutions of Tyr^6 and Leu^7 were found to have less of a stimulatory effect on SERCA maximal activity (37). Thus, the residue changes at these two positions (Tyr^6 to His and Leu^7 to Met) account for the functional

TABLE 2

Rate constants from kinetic simulations (s^{-1} ± S.E.)

* indicates one-sample *t* test significantly different from previously reported rate constants (21), $p < 0.01$. ** indicates one-sample *t* test significantly different from rate constants for SERCA alone, $p < 0.01$. *** indicates one-sample *t* test significantly different from rate constants for both SERCA alone and SERCA in the presence of PLN, $p < 0.01$. All other rate constants were not significantly different and were fixed at the reported rate constant values (21).

Rate constant[a]	Reconstituted proteoliposomes				
	SERCA[b]	PLN	SLN	zfPLN	zfPLN(−5)
A_{for}	190,700 ± 600*	190,000	157,200 ± 700***	119,500 ± 400***	114,800 ± 400***
A_{rev}	400	400	64,000 ± 600***	34,900 ± 400***	400
Ratio[c]	477	475	2.5	3.4	287
B_{rev}	40	26,000 ± 1000**	132,000 ± 4000***	92,000 ± 3000***	15,000 ± 4000***
Ratio[c]	0.75	0.00172	0.000167	0.00056	0.0035
C_{for}	1,810,000 ± 40,000*	250,000 ± 2000**	1,810,000	1,810,000	1,810,000
C_{rev}	16	16	16	16	16
Ratio[c]	113,125	15,625	113,125	113,125	113,125
SSR[d]	0.002	0.004	0.001	0.001	0.005

[a] Only rate constants with S.E. values were allowed to vary during the kinetic simulations. See "Experimental Procedures" for further details.
[b] Rate constants for SERCA in the absence of PLN (updated values from Trieber *et al.* (36)); these rate constants are used as the starting point for kinetic simulations of SERCA in the presence of PLN, SLN, zfPLN, and zfPLN(−5).
[c] A_{for} was divided by A_{rev}; B_{for} was divided by B_{rev}; and C_{for} was divided by C_{rev}.
[d] Sum of squared residuals (SSR); minimization of the sum of squared residuals between the kinetic model and experimental data is shown.

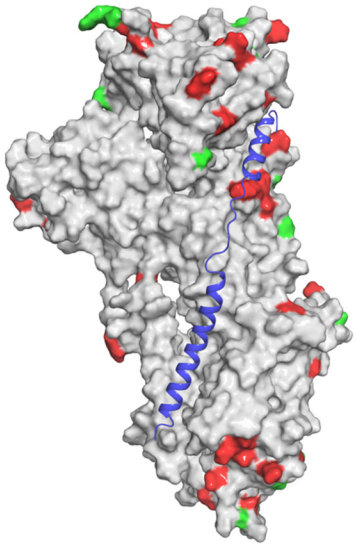

FIGURE 9. **Sequence variation between human and zebrafish SERCA2a and rabbit SERCA1a.** Surface representation of SERCA1a (*gray*) with the non-conservative amino acid variations between the human SERCA2a and rabbit SERCA1a shown in *red* and the zebrafish SERCA2a and rabbit SERCA1a shown in *green*. PLN is shown as a *blue ribbon* diagram.

consequences of the zfHEAD chimera. The effect of PLN on the maximal activity of SERCA is only observed at high protein to lipid and PLN to SERCA ratios that mimic cardiac SR membranes (36, 47), and this effect is not reversed by PKA-mediated phosphorylation (30). Residues that contribute to the V_{max} stimulation of SERCA are found in the cytoplasmic and transmembrane domains of PLN (30, 36, 37). In addition, the transmembrane domain of PLN by itself does not stimulate SERCA activity (40). Presumably then, SERCA interactions and coupling between the cytoplasmic and transmembrane domains of PLN underlie the effect on maximal activity.

There are two competing models for how the cytoplasmic domain of PLN participates in SERCA inhibition. In a recent model, the cytoplasmic domain of PLN does not interact with SERCA in the inhibitory complex, instead it adopts either a membrane-associated helix or a disordered state (48). In the prior models for the SERCA-PLN inhibitory complex (49, 50), Tyr^{6} and Leu^{7} are proximal to the hinge region that connects the N- and P-domains of SERCA (Fig. 10). It is notable that such an interaction could impact the flexible interface between the N- and P-domains. Because this region undergoes large conformational changes during calcium transport, it suggests a possible mechanism for how PLN can influence the turnover rate of SERCA. It is also notable that these residue changes have context-dependent effects on SERCA. Zebrafish and human PLN stimulate the maximal activity of SERCA, whereas the zfHEAD chimera is unable to do so.

Zebrafish MIDDLE—The largest cluster of residue changes between zebrafish and human PLN occurs in the linker region and extends into the N-terminal part of the transmembrane helix (Ile^{18} to Met, Met^{20} to Val, Arg^{25} to Lys, Lys^{27} to Asn, Leu^{28} to Met, Asn^{30} to Glu, and Ile^{33} to Val; Fig. 4). Although the residue changes are mainly conservative, there are several essential residues in this region of PLN. A zfMID chimera with these seven substitutions on the wild-type human background resulted in gain of inhibitory function and a more pronounced shift in the apparent calcium affinity of SERCA (Fig. 4 and Table 1). Thus, despite the conservative nature of the residue differences in zfPLN, one or more of the changes in the chimera altered human PLN function.

It has been proposed that polarity or positive charge in the linker region of PLN modulates the interaction with SERCA by destabilizing the SERCA-PLN inhibitory complex (49). Residues such as Lys^{27} and Asn^{30} of PLN are thought to be important for reducing the binding affinity such that SERCA inhibition occurs over a narrow range of calcium concentrations. In prior studies, alanine substitution of Ile^{18}, Met^{20}, Arg^{25} or Ile^{28} had little impact on PLN function (20), suggesting that the conservative substitutions found at these positions in zfPLN are unlikely to alter function. However, alanine substitution of Asn^{27} (rabbit PLN; Lys^{27} in humans), Asn^{30}, or Ile^{33} resulted in gain of function (super-inhibition of SERCA). Thus, one or more of these latter three residues are responsible for the zfMID gain of function. The gain of function previously observed for an Ile^{33} to Ala mutant was attributed to disruption of the PLN pentamer (24). Herein, the zfMID chimera harbor-

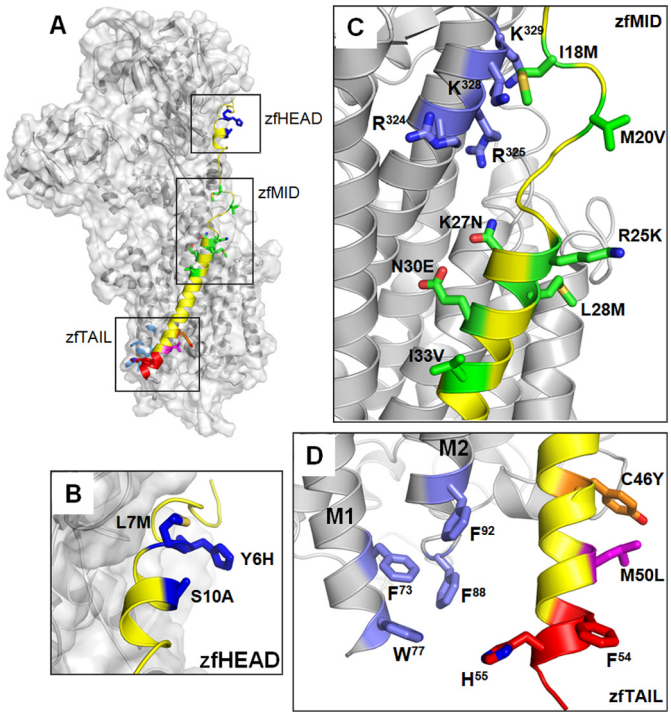

FIGURE 10. **Interactions between zfPLN and SERCA.** *A,* to understand changes in the cytoplasmic domain of zfPLN, a molecular model for the interaction with SERCA is shown (50). Residues that differ from the human PLN sequence are shown in *stick* representation and are color-coded. The *boxes* indicate the relative positions of the zfHEAD, zfMID, and zfTAIL chimeras. *B,* close-up view of the zfHEAD chimera based on the molecular model. *C,* close-up view of the zfMID chimera based on the reported structure of the SERCA-PLN complex (12) and the molecular model (50). *D,* close-up view of the zfTAIL chimera based on the reported structure of the SERCA-PLN complex (12). Phe^{54} and His^{55} (*red*) are in proximity to the luminal end of M1-M2 of SERCA (particularly Phe^{88} and Phe^{92}, which are in *light blue*). The zfTAIL region of zfPLN is shown as a continuous α-helix, although we anticipate that it may be partially unwound in the SERCA-PLN inhibitory complex.

ing the Ile^{33} to Val mutation was pentameric, indicating that this residue change is not responsible for the gain of function behavior of the chimera. Molecular models for the inhibitory complex place Lys^{27} and Asn^{30} of PLN proximal to a positively charged cluster of residues on SERCA (Fig. 10). In the reported structure of the SERCA-PLN complex (12), Lys^{27} and Asn^{30} have been mutated to alanine and cysteine, respectively, and these two residues sit below the positive charge cluster on SERCA. Nonetheless, Lys^{27} in human PLN is an asparagine in zfPLN and most mammalian species, so it is unlikely that this change has an effect on SERCA inhibition. With this in mind, the Asn^{30} to Glu substitution must modulate the binding affinity of PLN and cause super-inhibition of SERCA (Fig. 10). The glutamate substitution at this position validates the hypothesis that Asn^{30} is proximal to several positively charged residues in SERCA. As noted above for the zfHEAD chimera, there is a context-dependent effect of the Asn^{30} to Glu substitution. Zebrafish and human PLN have similar effects on SERCA activity, whereas the zfMID chimera results in super-inhibition.

Zebrafish Transmembrane Domain—The few residues in the transmembrane domain of zfPLN that differ from the human sequence are Cys^{46} to Tyr, Met^{50} to Leu, and Leu^{52} to Ile. The most interesting of these residue changes is the aromatic Tyr^{46} in zfPLN, which is reminiscent of the tryptophan residue at the homologous position in SLN (Trp^{23}; Fig. 1). Herein a Cys^{46} to Tyr mutant of human PLN had wild-type like properties even though it was unable to form stable pentamers by SDS-PAGE. In the available models for the PLN pentamer, Cys^{46} faces outward into the hydrocarbon core of the lipid bilayer (16, 51). It is known that the PLN pentamer is stabilized by a leucine-isoleucine zipper and that mutation of any of these residues destabilizes the pentamer and increases the prevalence of the monomeric form (24, 52). However, the three cysteine residues in the transmembrane domain of PLN also appear to be important for pentamer stability (53). Therefore, it may not be surprising that replacement of Cys^{46} with a tyrosine destabilizes the human PLN pentamer. In addition, it is intriguing that zfPLN, harboring Tyr^{46}, still forms pentamers. It should be noted that the luminal extension of zfPLN does not play a role in pentamer formation, as the tailless truncation constructs still form pentamers (data not shown). Thus, given that both zfPLN and SLN have an aromatic residue at this position (Tyr^{46} and Trp^{23}, respectively), examination of their sequences provides insight into determinants for pentamer formation. In zfPLN, the tendency of Tyr^{46} to destabilize the pentamer must be offset by compensatory features that allow oligomerization. Based on the available PLN sequences, the presence of Tyr^{46} is usually accompanied by Val^{33} and Leu^{50}, which are Ile^{33} and Met^{50} in human PLN (Fig. 1). These latter residues are required for pentamer formation (23, 24), and the conservative amino acid changes in zfPLN may serve to accommodate the disruptive contributions of Tyr^{46}. In addition, SLN has a charged residue (Arg^{27}) at the equivalent position of Met^{50} in human PLN, which may further destabilize the oligomeric forms in the case of SLN.

Zebrafish TAIL—In mammals and birds, the C terminus of PLN is a perfectly conserved structural and functional domain (Met^{50}-Leu-Leu^{52}; Fig. 1). However, the C terminus of zebrafish PLN isoform 2b contains five additional residues that are reminiscent of the luminal extension of SLN, a highly conserved structural and functional domain unique to this protein. Because this could suggest convergent evolution of SLN and zfPLN, we were interested in the potential function of this unique domain. For SLN, the luminal domain plays a role in SR retention and SERCA inhibition (8, 44, 54), and this contrasts with what is known for PLN. PLN lacks a luminal domain, and SR retention occurs via the di-arginine motif in its cytoplasmic domain (55). Because the di-arginine motif is conserved in zfPLN, it seems unlikely that its luminal domain would perform the redundant task. Thus, the question was whether the luminal domain of zfPLN makes a contribution to its inhibitory activity.

In our studies of SLN, removal of its luminal extension resulted in severe loss of inhibitory function (8). Similarly, the zfPLN truncation variants lost much of their ability to inhibit SERCA (~60% of the inhibitory capacity of full-length zfPLN). Thus, the luminal extension of zfPLN contributes to SERCA inhibition, and this is in marked contrast to all other known PLN homologs. Importantly, there was little difference between the two truncation variants (zfPLN(−5) and zfPLN(−6)), indicating that Ile^{52} does not contribute to the function of this domain. The luminal extension of SLN was also shown to be a distinct and transferable regulatory domain (8), and we

wondered whether the same was true for the zfPLN luminal domain. We found that the zfPLN luminal domain had only a minor effect on human PLN inhibitory function (Table 1). Thus, the luminal extension of zfPLN did not retain its functional properties when added to the C terminus of human PLN. Similarly, the luminal domain of zfPLN (^{53}SFHGM) could not be replaced by the luminal domain of SLN (^{27}RSYQY; Fig. 7). Instead, a zfPLN chimera containing the luminal extension of SLN resulted in potent super-inhibition of SERCA (Table 1), consistent with a previous study of this domain (8). Thus, the luminal domain of zfPLN has functional properties distinct from both PLN and SLN, and it can only regulate SERCA in the context of the primary structure of the full-length zebrafish protein.

Zebrafish PLN Uses a Hybrid Inhibitory Mechanism—Given the sequence variations in zfPLN, one would expect some unique functional characteristics to accompany these changes. Herein, we examined changes of a single residue (*e.g.* Cys^{46} to Tyr) or groups of residues (*e.g.* zfHEAD and zfMID) in the background of human PLN. It is clear from our results that sequence context matters. Therefore, despite mostly conservative sequence changes throughout its primary structure, residues such as Glu^{30} and Tyr^{46} gave rise to normal PLN function in zebrafish and aberrant functional properties when present in human PLN. An excellent example of this is the unique luminal extension, which contributes to zfPLN inhibitory function but does not contribute to function when added to human PLN. Thus, one conclusion is that the sequence variations among the different PLN homologs are balanced in a way that results in an almost identical PLN functional profile.

Comparing the linear sequences of PLN and SLN across species, the luminal extensions consist of three to eight residues as follows: ^{50}MLL in human PLN, ^{27}RSYQY in human SLN, and ^{50}LLISFHGM in zfPLN (Fig. 1). At first glance, zfPLN appears to contain a concatenation of typical PLN and SLN luminal extensions. The last five residues (^{53}SFHGM) are reminiscent of SLN, yet they are offset further into the lumen by three preceding residues (^{50}LLI) that are reminiscent of mammalian PLNs. These latter three residues are homologous to the highly conserved C terminus found in mammals and birds (^{50}MLL), whereas the two aromatic residues in zfPLN (Phe^{54} and His^{55}) may align with the terminal Tyr^{29} and Tyr^{31} of SLN. Both Tyr^{29} and Tyr^{31} of human SLN are important for SERCA inhibition, and they result in loss of function when mutated to alanine (8). We find that Phe^{54} and His^{55} of zfPLN are also important for SERCA inhibition, yet they result in gain of function when mutated to alanine (Table 1). This indicates a fundamental difference in the way luminal sequences modulate PLN and SLN function. A luminal domain is required for SLN function (8), yet it is absent (not required) for most homologs of PLN. In the case of PLN in zebrafish, isoform 2b possesses typical SERCA inhibitory capacity, whereas isoform 2a lacks the luminal domain and results in weaker SERCA inhibition. We conclude that the zfPLN luminal domain contributes to SERCA inhibition, while carefully avoiding super-inhibition.

In the structure of the SERCA-SLN complex (10, 11), Tyr^{29} of SLN is proximal to Phe^{88} on M2 of SERCA, although Arg^{27} and Tyr^{31} face away from SERCA. These latter two residues are positioned to protrude into the membrane at the hydrocarbon core-water interface, thereby acting as ballast to properly position SLN in the inhibitory complex (Fig. 10). Phe^{54} and His^{55} of zfPLN may play a similar role in positioning zfPLN in the inhibitory complex. As a result, the complex sequence variations throughout zfPLN result in different levels of SERCA inhibition in the absence (zfPLN isoform 2a) or presence (zfPLN isoform 2b) of the luminal tail. Although this domain superficially resembles that found in SLN, it uses distinct structural features to achieve optimal SERCA inhibition.

Although mammalian and zebrafish PLNs have similar inhibitory capacities, it is reasonable to expect that their distinct structural features result in mechanistic differences in the way they regulate SERCA. Indeed, there are clear differences in the ATPase activity isotherms for SERCA in the presence of zebrafish *versus* human PLN (Fig. 2*E*). Although the apparent calcium affinity of SERCA is similar, the curve shapes indicate significantly higher cooperativity for calcium binding in the presence of human PLN. This is because PLN alters a conformational transition in SERCA that follows binding of the first calcium ion, which in turn increases the cooperativity for binding of the second calcium ion (21, 36). Zebrafish PLN targets this same step, yet it also alters the binding of the first calcium ion to SERCA (Table 2). This latter effect is entirely encoded by the luminal extension of zfPLN, and it is reminiscent of the mechanism used by SLN (8). However, the luminal extensions of zfPLN and SLN are distinct domains, even though they achieve a similar mechanistic result in regulating SERCA. With PLN primarily using its transmembrane domain to regulate SERCA and SLN primarily relying on its luminal domain, zfPLN uses a hybrid PLN-SLN mechanism with contributions from both domains.

Finally, an interesting feature of the zebrafish genome is that it encodes multiple PLN isoforms. Although gene duplication is common in fish (56), the isoforms differ in their primary structures (Fig. 1). Isoform 2b has the unique luminal domain and isoforms 1 and 2a lack this domain and more closely resemble human PLN. Because the zfPLN luminal domain contributes to SERCA inhibition, the isoforms also differ in their inhibitory capacity. To the best of our knowledge, this is the first example of an organism with distinct PLN variants. It raises the interesting possibility that SR calcium handling and cardiac contractility may be regulated by the differential expression of PLN variants with different SERCA inhibitory capacities.

REFERENCES

1. Kirchberber, M. A., Tada, M., and Katz, A. M. (1975) Phospholamban: a regulatory protein of the cardiac sarcoplasmic reticulum. *Recent Adv. Stud. Cardiac Struct. Metab.* **5,** 103–115
2. Simmerman, H. K., Collins, J. H., Theibert, J. L., Wegener, A. D., and Jones, L. R. (1986) Sequence analysis of phospholamban. Identification of phosphorylation sites and two major structural domains. *J. Biol. Chem.* **261,** 13333–13341
3. Katz, A. M., Tada, M., and Kirchberger, M. A. (1975) Control of calcium transport in the myocardium by the cyclic AMP–protein kinase system. *Adv. Cyclic Nucleotide Res.* **5,** 453–472
4. Odermatt, A., Becker, S., Khanna, V. K., Kurzydlowski, K., Leisner, E., Pette, D., and MacLennan, D. H. (1998) Sarcolipin regulates the activity of SERCA1, the fast-twitch skeletal muscle sarcoplasmic reticulum Ca^{2+}-ATPase. *J. Biol. Chem.* **273,** 12360–12369

5. Wawrzynow, A., Theibert, J. L., Murphy, C., Jona, I., Martonosi, A., and Collins, J. H. (1992) Sarcolipin, the "proteolipid" of skeletal muscle sarcoplasmic reticulum, is a unique, amphipathic, 31-residue peptide. *Arch. Biochem. Biophys.* **298,** 620–623
6. Asahi, M., Sugita, Y., Kurzydlowski, K., De Leon, S., Tada, M., Toyoshima, C., and MacLennan, D. H. (2003) Sarcolipin regulates sarco(endo)plasmic reticulum Ca^{2+}-ATPase (SERCA) by binding to transmembrane helices alone or in association with phospholamban. *Proc. Natl. Acad. Sci. U.S.A.* **100,** 5040–5045
7. Morita, T., Hussain, D., Asahi, M., Tsuda, T., Kurzydlowski, K., Toyoshima, C., and Maclennan, D. H. (2008) Interaction sites among phospholamban, sarcolipin, and the sarco(endo)plasmic reticulum Ca^{2+}-ATPase. *Biochem. Biophys. Res. Commun.* **369,** 188–194
8. Gorski, P. A., Glaves, J. P., Vangheluwe, P., and Young, H. S. (2013) Sarco-(endo)plasmic reticulum calcium ATPase (SERCA) inhibition by sarcolipin is encoded in its luminal tail. *J. Biol. Chem.* **288,** 8456–8467
9. Bal, N. C., Maurya, S. K., Sopariwala, D. H., Sahoo, S. K., Gupta, S. C., Shaikh, S. A., Pant, M., Rowland, L. A., Bombardier, E., Goonasekera, S. A., Tupling, A. R., Molkentin, J. D., and Periasamy, M. (2012) Sarcolipin is a newly identified regulator of muscle-based thermogenesis in mammals. *Nat. Med.* **18,** 1575–1579
10. Winther, A. M., Bublitz, M., Karlsen, J. L., Møller, J. V., Hansen, J. B., Nissen, P., and Buch-Pedersen, M. J. (2013) The sarcolipin-bound calcium pump stabilizes calcium sites exposed to the cytoplasm. *Nature* **495,** 265–269
11. Toyoshima, C., Iwasawa, S., Ogawa, H., Hirata, A., Tsueda, J., and Inesi, G. (2013) Crystal structures of the calcium pump and sarcolipin in the Mg^{2+}-bound E1 state. *Nature* **495,** 260–264
12. Akin, B. L., Hurley, T. D., Chen, Z., and Jones, L. R. (2013) The structural basis for phospholamban inhibition of the calcium pump in sarcoplasmic reticulum. *J. Biol. Chem.* **288,** 30181–30191
13. Traaseth, N. J., Shi, L., Verardi, R., Mullen, D. G., Barany, G., and Veglia, G. (2009) Structure and topology of monomeric phospholamban in lipid membranes determined by a hybrid solution and solid-state NMR approach. *Proc. Natl. Acad. Sci. U.S.A.* **106,** 10165–10170
14. Lamberth, S., Schmid, H., Muenchbach, M., Vorherr, T., Krebs, J., Carafoli, E., and Griesinger, C. (2000) NMR solution structure of phospholamban. *Helv. Chim. Acta* **83,** 2141–2152
15. Mortishire-Smith, R. J., Pitzenberger, S. M., Burke, C. J., Middaugh, C. R., Garsky, V. M., and Johnson, R. G. (1995) Solution structure of the cytoplasmic domain of phospholamban: phosphorylation leads to a local perturbation of secondary structure. *Biochemistry* **34,** 7603–7613
16. Oxenoid, K., and Chou, J. (2005) The structure of phospholamban pentamer reveals a channel-like architecture in membranes. *Proc. Natl. Acad. Sci. U.S.A.* **102,** 10870–10875
17. Haghighi, K., Kolokathis, F., Gramolini, A. O., Waggoner, J. R., Pater, L., Lynch, R. A., Fan, G. C., Tsiapras, D., Parekh, R. R., Dorn, G. W., 2nd, MacLennan, D. H., Kremastinos, D. T., and Kranias, E. G. (2006) A mutation in the human phospholamban gene, deleting arginine 14, results in lethal, hereditary cardiomyopathy. *Proc. Natl. Acad. Sci. U.S.A.* **103,** 1388–1393
18. Medeiros, A., Biagi, D. G., Sobreira, T. J., de Oliveira, P. S., Negrão, C. E., Mansur, A. J., Krieger, J. E., Brum, P. C., and Pereira, A. C. (2011) Mutations in the human phospholamban gene in patients with heart failure. *Am. Heart J.* **162,** 1088–1095
19. Schmitt, J. P., Kamisago, M., Asahi, M., Li, G. H., Ahmad, F., Mende, U., Kranias, E. G., MacLennan, D. H., Seidman, J. G., and Seidman, C. E. (2003) Dilated cardiomyopathy and heart failure caused by a mutation in phospholamban. *Science* **299,** 1410–1413
20. Kimura, Y., Asahi, M., Kurzydlowski, K., Tada, M., and MacLennan, D. H. (1998) Phospholamban domain Ib mutations influence functional interactions with the Ca^{2+}-ATPase isoform of cardiac sarcoplasmic reticulum. *J. Biol. Chem.* **273,** 14238–14241
21. Cantilina, T., Sagara, Y., Inesi, G., and Jones, L. R. (1993) Comparative studies of cardiac and skeletal sarcoplasmic reticulum ATPases: effect of phospholamban antibody on enzyme activation. *J. Biol. Chem.* **268,** 17018–17025
22. Kimura, Y., Kurzydlowski, K., Tada, M., and MacLennan, D. H. (1996) Phospholamban regulates the Ca^{2+}-ATPase through intramembrane interactions. *J. Biol. Chem.* **271,** 21726–21731
23. Simmerman, H. K., Kobayashi, Y. M., Autry, J. M., and Jones, L. R. (1996) A leucine zipper stabilizes the pentameric membrane domain of phospholamban and forms a coiled-coil pore structure. *J. Biol. Chem.* **271,** 5941–5946
24. Kimura, Y., Kurzydlowski, K., Tada, M., and MacLennan, D. H. (1997) Phospholamban inhibitory function is enhanced by depolymerization. *J. Biol. Chem.* **272,** 15061–15064
25. Gramolini, A. O., Trivieri, M. G., Oudit, G. Y., Kislinger, T., Li, W., Patel, M. M., Emili, A., Kranias, E. G., Backx, P. H., and Maclennan, D. H. (2006) Cardiac-specific overexpression of sarcolipin in phospholamban null mice impairs myocyte function that is restored by phosphorylation. *Proc. Natl. Acad. Sci. U.S.A.* **103,** 2446–2451
26. Bhupathy, P., Babu, G. J., Ito, M., and Periasamy, M. (2009) Threonine-5 at the N terminus can modulate sarcolipin function in cardiac myocytes. *J. Mol. Cell. Cardiol.* **47,** 723–729
27. Will, H., Küttner, I., Vetter, R., Will-Shahab, L., and Kemsies, C. (1983) Early presence of phospholamban in developing a chick heart. *FEBS Lett.* **155,** 326–330
28. Will, H., Küttner, I., Kemsies, C., Vetter, R., and Schubert, E. (1985) Comparative analysis of phospholamban phosphorylation in crude membranes of vertebrate hearts. *Experientia* **41,** 1052–1054
29. Douglas, J. L., Trieber, C. A., Afara, M., and Young, H. S. (2005) Rapid, high-yield expression and purification of Ca^{2+}-ATPase regulatory proteins for high-resolution structural studies. *Protein Expr. Purif.* **40,** 118–125
30. Trieber, C. A., Douglas, J. L., Afara, M., and Young, H. S. (2005) The effects of mutation on the regulatory properties of phospholamban in co-reconstituted membranes. *Biochemistry* **44,** 3289–3297
31. Eletr, S., and Inesi, G. (1972) Phospholipid orientation in sarcoplasmic membranes: spin-label ESR and proton MNR studies. *Biochim. Biophys. Acta* **282,** 174–179
32. Stokes, D. L., and Green, N. M. (1990) Three-dimensional crystals of CaATPase from sarcoplasmic reticulum. Symmetry and molecular packing. *Biophys. J.* **57,** 1–14
33. Reddy, L. G., Jones, L. R., Pace, R. C., and Stokes, D. L. (1996) Purified, reconstituted cardiac Ca^{2+}-ATPase is regulated by phospholamban but not by direct phosphorylation with Ca^{2+}/calmodulin-dependent protein kinase. *J. Biol. Chem.* **271,** 14964–14970
34. Young, H. S., Jones, L. R., and Stokes, D. L. (2001) Locating phospholamban in co-crystals with Ca^{2+}-ATPase by cryoelectron microscopy. *Biophys J* **81,** 884–894
35. Warren, G. B., Toon, P. A., Birdsall, N. J., Lee, A. G., and Metcalfe, J. C. (1974) Reconstitution of a calcium pump using defined membrane components. *Proc. Natl. Acad. Sci. U.S.A.* **71,** 622–626
36. Trieber, C. A., Afara, M., and Young, H. S. (2009) Effects of phospholamban transmembrane mutants on the calcium affinity, maximal activity, and cooperativity of the sarcoplasmic reticulum calcium pump. *Biochemistry* **48,** 9287–9296
37. Ceholski, D. K., Trieber, C. A., and Young, H. S. (2012) Hydrophobic imbalance in the cytoplasmic domain of phospholamban is a determinant for lethal dilated cardiomyopathy. *J. Biol. Chem.* **287,** 16521–16529
38. Inesi, G., Kurzmack, M., and Lewis, D. (1988) Kinetic and equilibrium characterization of an energy-transducing enzyme and its partial reactions. *Methods Enzymol.* **157,** 154–190
39. Afara, M. R., Trieber, C. A., Ceholski, D. K., and Young, H. S. (2008) Peptide inhibitors use two related mechanisms to alter the apparent calcium affinity of the sarcoplasmic reticulum calcium pump. *Biochemistry* **47,** 9522–9530
40. Afara, M. R., Trieber, C. A., Glaves, J. P., and Young, H. S. (2006) Rational design of peptide inhibitors of the sarcoplasmic reticulum calcium pump. *Biochemistry* **45,** 8617–8627
41. Ceholski, D. K., Trieber, C. A., Holmes, C. F., and Young, H. S. (2012) Lethal, hereditary mutants of phospholamban elude phosphorylation by protein kinase A. *J. Biol. Chem.* **287,** 26596–26605
42. Fujii, J., Maruyama, K., Tada, M., and MacLennan, D. H. (1989) Expression and site-specific mutagenesis of phospholamban: studies of residues in-

volved in phosphorylation and pentamer formation. *J. Biol. Chem.* **264,** 12950–12955
43. Glaves, J. P., Trieber, C. A., Ceholski, D. K., Stokes, D. L., and Young, H. S. (2011) Phosphorylation and mutation of phospholamban alter physical interactions with the sarcoplasmic reticulum calcium pump. *J. Mol. Biol.* **405,** 707–723
44. Hughes, E., Clayton, J. C., Kitmitto, A., Esmann, M., and Middleton, D. A. (2007) Solid-state NMR and functional measurements indicate that the conserved tyrosine residues of sarcolipin are involved directly in the inhibition of SERCA1. *J. Biol. Chem.* **282,** 26603–26613
45. Vandecaetsbeek, I., Trekels, M., De Maeyer, M., Ceulemans, H., Lescrinier, E., Raeymaekers, L., Wuytack, F., and Vangheluwe, P. (2009) Structural basis for the high Ca^{2+} affinity of the ubiquitous SERCA2b Ca^{2+} pump. *Proc. Natl. Acad. Sci. U.S.A.* **106,** 18533–18538
46. Gorski, P. A., Trieber, C. A., Larivière, E., Schuermans, M., Wuytack, F., Young, H. S., and Vangheluwe, P. (2012) Transmembrane helix 11 is a genuine regulator of the endoplasmic reticulum Ca^{2+} pump and acts as a functional parallel of β-subunit on α-Na^+,K^+-ATPase. *J. Biol. Chem.* **287,** 19876–19885
47. Reddy, L. G., Cornea, R. L., Winters, D. L., McKenna, E., and Thomas, D. D. (2003) Defining the molecular components of calcium transport regulation in a reconstituted membrane system. *Biochemistry* **42,** 4585–4592
48. Gustavsson, M., Verardi, R., Mullen, D. G., Mote, K. R., Traaseth, N. J., Gopinath, T., and Veglia, G. (2013) Allosteric regulation of SERCA by phosphorylation-mediated conformational shift of phospholamban. *Proc. Natl. Acad. Sci. U.S.A.* **110,** 17338–17343
49. Toyoshima, C., Asahi, M., Sugita, Y., Khanna, R., Tsuda, T., and MacLennan, D. (2003) Modeling of the inhibitory interaction of phospholamban with the Ca^{2+} ATPase. *Proc. Natl. Acad. Sci. U.S.A.* **100,** 467–472
50. Seidel, K., Andronesi, O. C., Krebs, J., Griesinger, C., Young, H. S., Becker, S., and Baldus, M. (2008) Structural characterization of Ca^{2+}-ATPase-bound phospholamban in lipid bilayers by solid-state nuclear magnetic resonance (NMR) spectroscopy. *Biochemistry* **47,** 4369–4376
51. Verardi, R., Shi, L., Traaseth, N. J., Walsh, N., and Veglia, G. (2011) Structural topology of phospholamban pentamer in lipid bilayers by a hybrid solution and solid-state NMR method. *Proc. Natl. Acad. Sci. U.S.A.* **108,** 9101–9106
52. Autry, J. M., and Jones, L. R. (1997) Functional co-expression of the canine cardiac Ca^{2+} pump and phospholamban in *Spodoptera frugiperda* (Sf21) cells reveals new insights on ATPase regulation. *J. Biol. Chem.* **272,** 15872–15880
53. Karim, C. B., Paterlini, M. G., Reddy, L. G., Hunter, G. W., Barany, G., and Thomas, D. D. (2001) Role of cysteine residues in structural stability and function of a transmembrane helix bundle. *J. Biol. Chem.* **276,** 38814–38819
54. Gramolini, A. O., Kislinger, T., Asahi, M., Li, W., Emili, A., and MacLennan, D. H. (2004) Sarcolipin retention in the endoplasmic reticulum depends on its C-terminal RSYQY sequence and its interaction with sarco(endo)plasmic Ca^{2+}-ATPases. *Proc. Natl. Acad. Sci. U.S.A.* **101,** 16807–16812
55. Sharma, P., Ignatchenko, V., Grace, K., Ursprung, C., Kislinger, T., and Gramolini, A. O. (2010) Endoplasmic reticulum protein targeting of phospholamban: a common role for an N-terminal di-arginine motif in ER retention? *PLoS One* **5,** e11496
56. Meyer, A., and Schartl, M. (1999) Gene and genome duplications in vertebrates: the one to four (to eight in fish) rule and the evolution of novel gene functions. *Curr. Opin. Cell Biol.* **11,** 699–704